



Version: v0.25 as of March 11, 2006
Primary author(s): A. Haas

Send comments to d0-run2eb-020@fnal.gov
by March 10, 2006

Search for Stopped Gluinos

A long-lived gluino is a generic prediction of several models of beyond the Standard Model physics, such as Split-SUSY. Some fraction of the hadronized gluinos (R-hadrons) would lose enough momentum to come to rest in the calorimeters, becoming stopped gluinos (G). About 350 pb^{-1} of Tevatron Run II $p\bar{p}$ data at $\sqrt{s} = 1960 \text{ GeV}$ collected by the DØ experiment is analyzed in search of stopped gluinos decaying into a single jet and a neutralino. No excess is observed above the expected background from cosmic-muon induced showers, and limits are placed on the stopped gluino cross-section $\times \text{BR}(G \rightarrow g\chi_1^0)$ as a function of the gluino and neutralino masses.

Preliminary Results for Winter 2006 Conferences

I. INTRODUCTION AND THEORY

Split-Supersymmetry is a relatively new variant of Supersymmetry, in which the Supersymmetric scalars are heavy (possibly GUT-scale) compared to the (SUSY) fermions [1]. This simple relaxation of one of the standard assumptions of Supersymmetry avoids many fine-tunings which must be incorporated to remain consistent with observations while still preserving the favored consequences. A dark-matter candidate is still present in the theory to explain the observed cold-dark matter density in the Universe, GUT-scale coupling unification still occurs, and the required Supersymmetry is still present as needed for String theory. Due to the scalars' high masses, the gluino decays are suppressed, and the gluino lifetime is determined by this SUSY-scalar mass scale (M_{SUSY}). The gluinos have time to hadronize into “R-hadrons”, colorless bound states of a gluino and other quarks or gluons.

At the Tevatron, R-hadrons could be pair produced through strong interactions. If $M_{SUSY} > 10^6$ GeV, the R-hadrons live long enough (>10 ns) to reach the DØ calorimeters. Recent hadronization models of gluinos [2] predict a spectrum with degenerate light meson-like states, and about 1/2 of R-hadrons being charged. R-hadrons can also become charged when passing through matter. As studied in [3], some charged R-hadrons can become “stopped gluinos”, by losing all of their momentum through ionization and coming to rest in the calorimeters. Most of these stopped gluinos would later decay into a jet (from a gluon) and a neutralino (LSP).

This analysis searches for stopped gluinos (G) produced at the Tevatron in Run II, decaying into a jet plus neutralino. The stopped gluino lifetime is assumed to be long enough such that the decay of the gluino occurs during a bunch-crossing later than the one which produced it (at least 10 μ s). The decay is also assumed to take place soon enough such that data is consistently being recorded during the decay, so the lifetime should be less than a few hours. When the decay occurs during a bunch-crossing with very little other high- p_T activity, the signal signature is a largely empty event with a single high- p_T jet and thus large missing E_T .

It is worth noting that several other interesting and more complicated related signatures are also available. When one of the pair-produced gluinos stops in the calorimeters, 30% of the time the other one stops as well [3], since the p_T of the two gluinos are highly correlated in each event. This makes possible the search for “double-bang” events, where two decays are observed close in time. Double-band events are a way to directly measure the gluino lifetime and thus M_{SUSY} . Another phenomenon is the two-jet decay plus MET, coming from the decay $G \rightarrow q\bar{q}\chi_1^0$, which may be possible to distinguish from the single-jet decay. The branching fraction of double- to single- jet decays would also provide information on M_{SUSY} . Finally, it may be possible to observe the decay $G \rightarrow \chi_2^0 j \rightarrow \chi_1^0 \mu^+ \mu^- j$ with two muons coming from the jet location with an invariant mass less than or equal to the mass difference of the two neutralinos. However, the search for and study of these processes will be left to future investigations.

II. SIMULATION

The stopped gluino decays a majority of the time into a gluon plus a neutralino (LSP). There is also some branching fraction to two quarks plus a neutralino, possibly up to 50% depending on various model parameters, but these decays will be ignored. The analysis specifically searches for mono-jet events (i.e. limits will be set on the cross-section \times BR to a gluon + LSP). The radial location of the gluino when it decays depends on the way the gluinos lose energy via ionization and stop in the calorimeters. This calculation was performed [3] for a distribution of material similar to the DØ calorimeters (production at the Tevatron). The $|\eta|$ distribution is determined by the fact that gluinos would tend to be produced near threshold at the Tevatron, and that only slow gluinos would stop. Therefore the gluinos are expected to be distributed proportional to $\cos\theta$, with more than 75% of gluinos stopping in $|\eta|<1$. The gluinos are at rest and randomly oriented in space when they decay; thus the gluon is emitted in a random direction. The energy of the gluon (jet) depends on the gluino and LSP masses:

$$E = (M_g^2 - M_{LSP}^2)/2M_g \quad (1)$$

To simulate the jets that would be produced by stopped gluino decays, Pythia was used to produce Z+gluon events (MSEL=13) with the Z forced to decay to neutrinos. The location of the interaction point (the gluino decay location) was set to (x,y,z)=(0 \pm 20,120 \pm 20,0 \pm 80) cm, near the outside of the EM calorimeter layers. The vertex is chosen in each event according to a Gaussian distribution in each coordinate. The 80 cm RMS of the z vertex location roughly corresponds to the $|\eta|$ distribution of the stopped gluinos, but events are further weighted such that the final event decay z locations are proportional to $\tanh\eta = \cos\theta$, as expected for stopped gluinos. Initial-state radiation (ISR) was switched off in Pythia, and so were multiple parton interactions, since we do not really want to simulate a full $p\bar{p}$ beam. The $|\eta|$ of the gluon was restricted to be less than 0.1 at the generator level. The spectator particles coming from the rest of the $p\bar{p}$ interaction, such as the underlying event, were removed at the generator stage by suppressing (setting momenta to 0.01) all particles with $|pz/E| > 0.95$. Finally, a random 3D rotation was applied to the remaining particles, to simulate the random decay axis of the gluino.

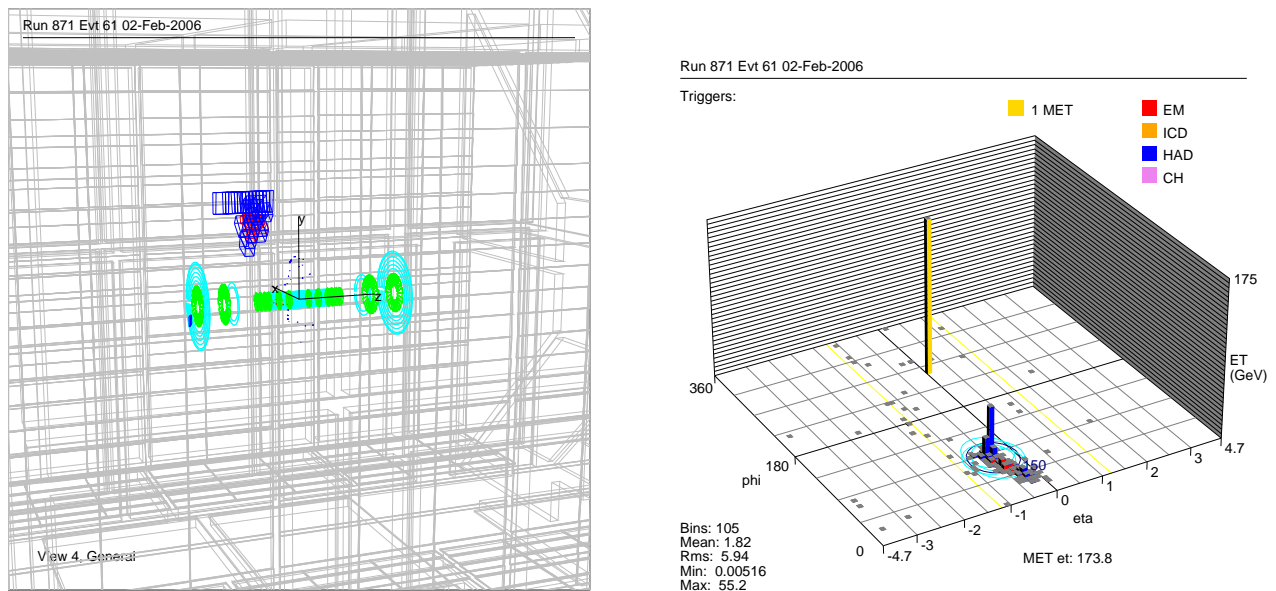


FIG. 1: A fairly typical simulated stopped gluino decay event, for $m_G=400$ GeV. The left figure shows a 3D view of the detector with the silicon tracker and outer muon chambers visible. The calorimeter cells with significant energy in the EM and Handronic layers are outlined in red and blue, respectively. Reconstructed tracks would be shown as black curves, but none were reconstructed. The right figure shows a Lego plot of the same event, where the height of each bar corresponds to the total E_T in that $\eta \times \phi$ tower. The \cancel{E}_T is shown as a yellow bar.

Four samples of “stopped gluino MC” were produced, containing 1000 events each. The samples had mass cuts at the generator level (CKIN(1)-(2) in Pythia), corresponding to gluino masses of 200, 300, 400, and 500 GeV, for an LSP mass of 90 GeV (the Z behaves similarly to an LSP of the same mass). Using Equation 1, we note that these samples thus correspond to generated parton (jet) energies of 80, 137, 190, and 242 GeV, respectively. A little more than half the gluino energy goes to the LSP. An event display of a simulated stopped gluino decay is shown in Figure 1.

III. DATA SAMPLE

Data taken from November 2002 – August 2004, about 350 pb^{-1} , were reconstructed and corrected with “p14 PASS2” software. Since no $p\bar{p}$ beam-interaction is expected to be correlated with the stopped gluino decay, the “DIFF” (designed for diffractive physics) skim was selected and one of the “GAPSN” triggers were required for each event. The GAPSN triggers require no firing of either the North or South luminosity counters, placed on the front face of the end-cap calorimeters at high $|\eta|$. Two versions exist, the first, JT_15TT_GAPSN, has lower calorimeter thresholds and is prescaled at some very high luminosities, and the second, JT_45TT_GAPSN, is always un-prescaled. The first trigger requires 2 L1 calorimeter towers above 3 GeV and a 15 GeV L3 jet. The second requires 2 L1 calorimeter towers above 5 GeV and a 45 GeV L3 jet. About 7.9 million events exist in the initial trigger-selected, skimmed, data sample.

IV. OBJECT IDENTIFICATION

Jets were reconstructed with the Run II Improved Legacy Cone Algorithm (ILCA) [4] with cone size of 0.5 (JCCB). Jets were not required to pass any quality criteria or corrected back to the particle level for detector and physics effects using jet energy scale factors, since the assumptions used to derive these corrections (a projective geometry, etc.) are not valid for these jets.

Muons were reconstructed and no extra quality criteria or corrections were applied. The $D\bar{O}$ muon detector system has three layers (A,B,C). The first (A) is inside the iron toroid magnet, while the second two (B,C) are outside it. Muons were separated according to whether they extended beyond the A-layer or not.

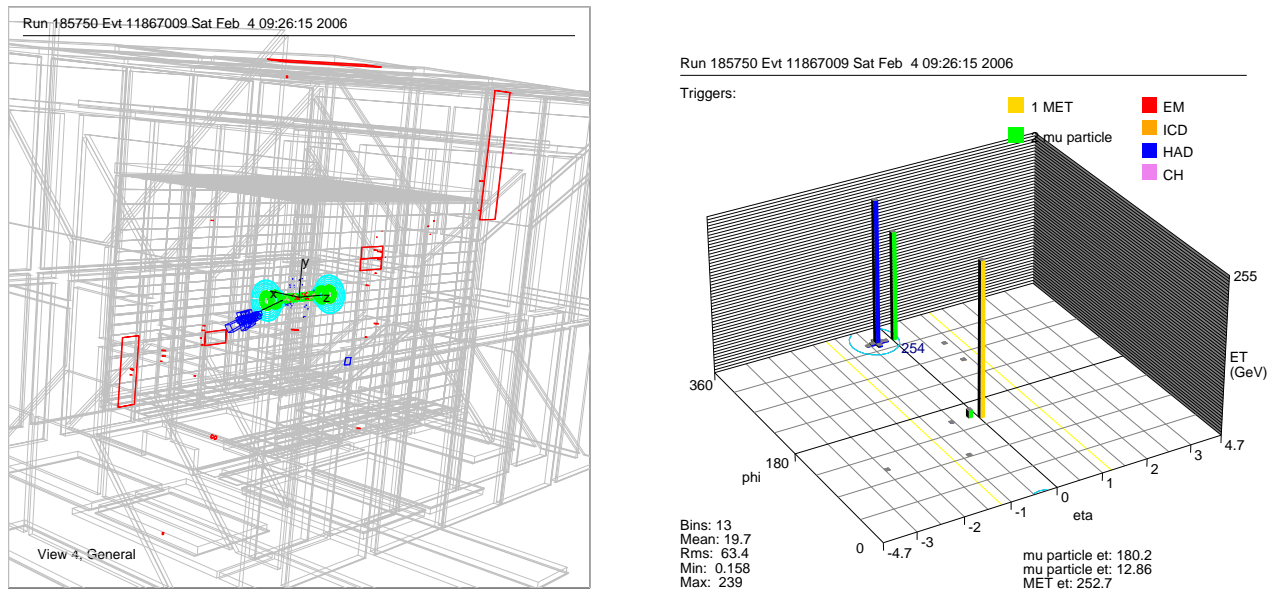


FIG. 2: A typical cosmic muon, hard Bremsstrahlung, shower. There are reconstructed muons (shown in green) and a very narrow energy deposit.

V. PRE-SELECTION

In addition to the trigger criteria described above, loose cuts were used to select an initial data sample to study.

- Require “good” muon and tracking runs, for rejection of cosmic and diffractive events.
- Require exactly one JCCB jet in the event. This helps to reduce certain kinds of detector noise, and also simplifies the analysis.
- Jet $E > 90$ GeV. This avoids noise jets and is also high enough such that the calorimeter part of the trigger is nearly 100% efficient.

VI. SOURCES OF BACKGROUND

The major source of background is cosmic muons, which are able to fake a gluino signal if they initiate a high-energy shower within the calorimeter. The rate for a cosmic muon to deposit enough energy to pass the pre-selection criteria is observed to be quite large, about 0.1 Hz. Hard bremsstrahlung emission is responsible for the majority of the showers. (The probability for a hard-photon of at least 10% of the muon energy to be created in 3m of iron is about 0.1%.) Fortunately, these showers tend to be very narrow, since they are electromagnetic in nature and thus have small interaction lengths compared to hadronic showers. Most of the energy is deposited in a few calorimeter cells, see Figure 2. However, sometimes a wide, hadronic-like, shower can be created either due to real deep-inelastic scattering, fluctuations of the shower, or detector effects. Cosmic muons can also mimic other, rarer, signal-like qualities, such as a large muon “A-layer splash” caused by part of the shower escaping the calorimeter and hitting the inner (A-layer) muon chambers.

Cosmic muons can usually be identified by the presence of a high-energy muon, either entering or exiting the detector, using the muon detectors. In particular, a coincidence of muon hits in the outer two (B,C) layers of the muon system are very strong evidence of a muon. The A-layer hits are often also caused by the signal, due to particles escaping the calorimeters, so these hits are difficult to use for background rejection. (These particles are nearly all absorbed in the iron toroid magnets before reaching the B,C layers, so do not cause signals often in these outer layers.) In fact, the A-layer hits are used if they are consistent with the geometry of a muon passing through the detector (back-to-back) and not near a hadronic shower. (See Section VII for complete description of these criteria.) However, sometimes the muon is not detected, due to detector inefficiencies or the limited detector acceptance up to $|\eta| < 2$. Muons can also be detected, in principle, through their ionizing interactions in the calorimeter, where they are minimum-ionizing particles (MIP’s). However, these MIP trails are difficult to identify in this geometry where

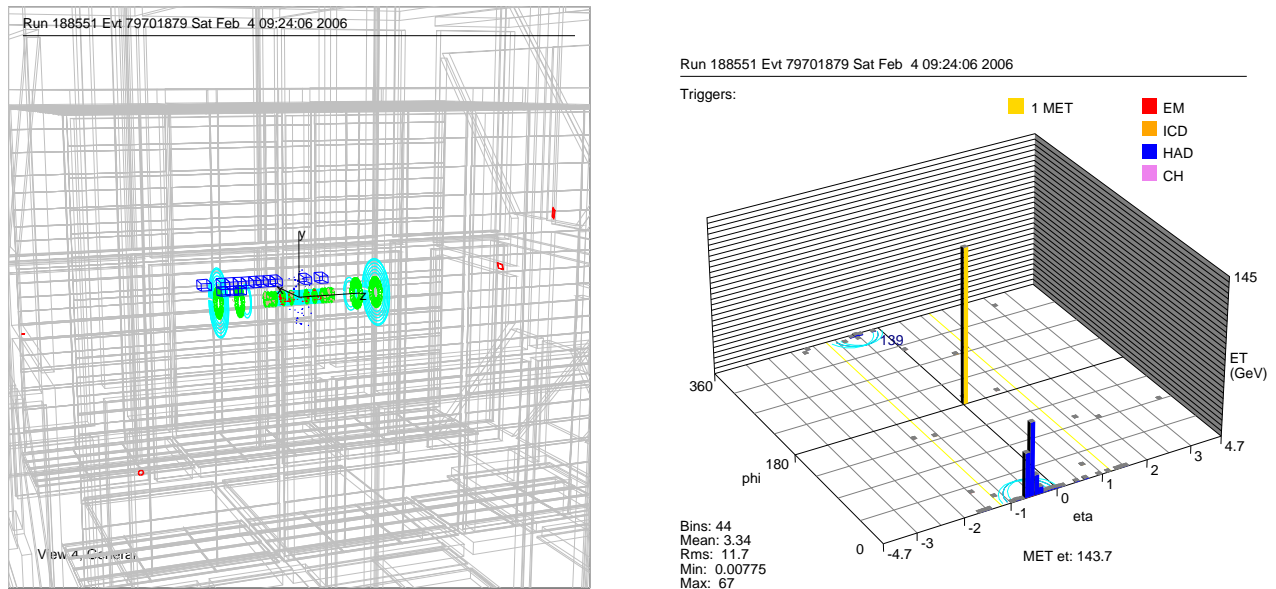


FIG. 3: A typical beam-muon shower. The jet is very narrow in ϕ , but long in η , and centered at an integer multiple of π (in the plane of the accelerator).

the direction of the muon path is unknown, and also there is a large shower nearby which overlaps with the energy deposited by the MIP.

Another source of background events is beam-halo muons, or “beam-muons”. These are muons, in-time with the $p\bar{p}$ bunches, and traveling nearly parallel to the beam, as seen in Figure 3. Often, a muon scintillator hit or two can be associated with the muon, and the muon can be seen to be in-time, with $\Delta t < 10$ ns. (Δt for a muon hit is the extent to which the hit is early or late, compared to a hit from a “standard muon”, traveling at speed c from the collision point.) Another feature of the beam-muons is that they are nearly all in the plane of the accelerator beam, i.e. with ϕ very near to integer multiples of π . This may be due to the geometry of accelerator magnets or collimators, or gaps in the shielding at either DØ or CDF. Beam-muon showers are also typically very narrow in ϕ -width, even narrower than cosmic muon showers. Since beam-muons are traveling parallel to the beam, the ϕ -width is small no matter how long the shower extends along the path of the muon. For the same reason, the η -width of beam-muons tends to be larger than for cosmic muons.

Since we are using the GAPSIN triggers, nearly all of the $p\bar{p}$ beam produced backgrounds are eliminated. An exception is double diffractive events with large momentum transfer. However, after requiring no primary vertex (PV) to be reconstructed and large \cancel{E}_T (implicit from the choice of only one central jet with $E > 90$ GeV), these events are eliminated. Di-jet events in the same data sample were studied to understand the \cancel{E}_T spectrum and PV reconstruction efficiency for beam-related backgrounds.

Other small sources of background considered are cosmic neutrons and neutrinos. Neutrons would be more effective in creating wide hadronic showers, but their rate is about 1/1000th that of cosmic muons of similar energy, and they also would be unlikely to penetrate the iron toroid magnets. In the event that one did reach the calorimeter, the neutron would most likely shower in the outer coarse-hadronic layer, which is not part of the L1 calorimeter trigger. Thus, we expect that the number of cosmic neutron events in the data sample is very low. Neutrinos are copious, but have a very low interaction rate. A back-of-the-envelope calculation predicts a neutrino-shower rate of about 0.1/year.

Finally, since the signal process is rare, one needs to consider the occasional fake signal processes caused by detector problems. However, these problems tend to be isolated to a specific set of runs, a specific detector region, or both.

VII. EVENT SELECTION

Now that the background sources are understood and the gluino signal is simulated, we can make selections to reduce the backgrounds while still remaining efficient for the gluino signal. We require:

- Jet $|\eta| < 0.9$. The forward regions of the calorimeter were observed to have some difficult detector problems. Also, the gluino signal tends to be concentrated in the central regions.

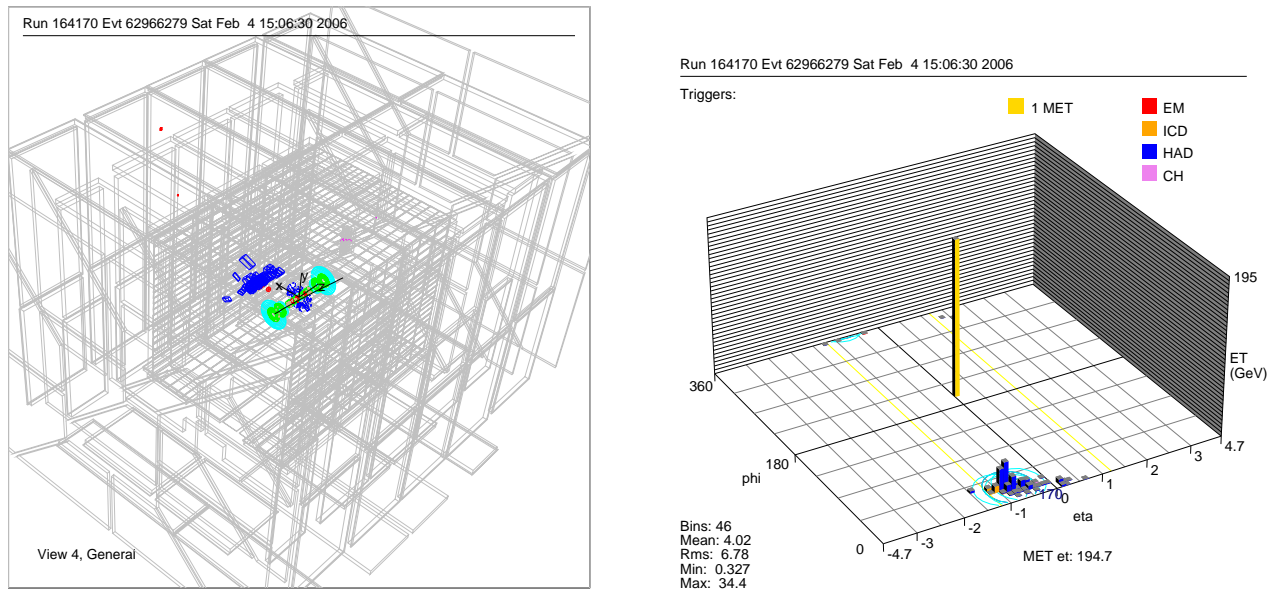


FIG. 4: A typical candidate signal event, containing a wide shower with no good muon.

- No reconstructed primary vertex (PV). This usually means that no tracks were reconstructed, although sometimes one or more tracks were reconstructed but did not form a vertex. This requirement removes background from diffractive events very effectively.
- The rectangular region of the calorimeter ($-.55 < \eta < -.75$, $1.3 < \phi < 1.5$) was too noisy and therefore all events in that region were rejected.
- Jet $E < 900$ GeV. This avoids certain kinds of detector problems and besides eliminates only un-physical gluinos at the Tevatron.
- Jet ϕ -width and η -width were both required to be < 0.25 to eliminate events from certain types of detector problems.

Further selections are then applied. The following criteria are used to select events containing “wide showers”. All jets which fail these cuts are considered “narrow jets”.

- Jet η -width and ϕ -width > 0.08 .
- Jet $n_{90} \geq 10$. (n_{90} is the smallest number of calorimeter cells in the jet that make up 90% of the jet energy.) This reduces contamination of fake wide showers from a narrow muon shower plus a long MIP trail.

The following criteria are used to select events containing “no-muon”. Events failing these criteria are considered “muon-jets”.

- No muons in the event extending beyond the A-layer. These events are nearly all cosmic muons (although we do lose about 10% efficiency here for gluino events).
- Require the $\Delta\phi$ between all pairs of A-layer-only muons to be < 1.5 . Gluino jets often leak into the A-layer a bit, but we want to veto on back-to-back A-layer muons that could come from a single cosmic muon.
- Require the $\Delta\phi$ between any A-layer-only muon and the jet to be < 1.5 . We want to allow the jet to leak into the A-layer, but veto events where the A-layer muon is not associated with the jet (since it is then likely to be due to a cosmic muon).

A candidate gluino shower would be both wide and contain no muon, a so-called “wide no-muon shower”. Figure 4 shows a display of a candidate event.

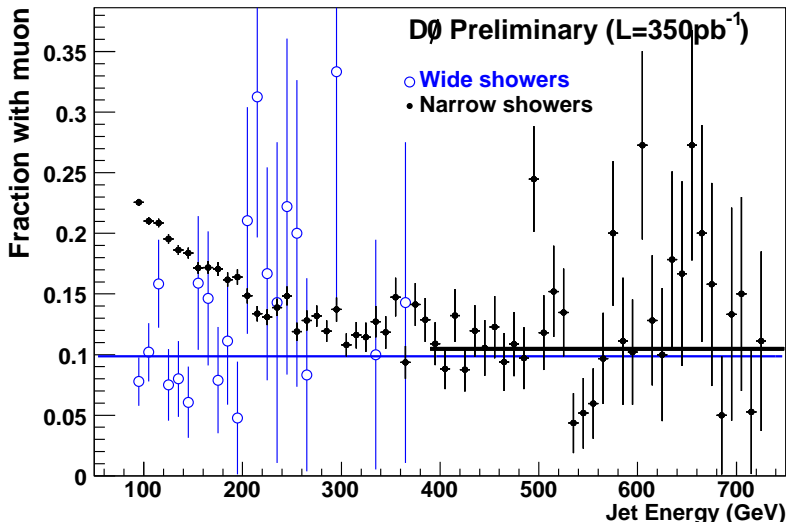


FIG. 5: The ratio of the number of wide (blue circles) and narrow (black dots) showers with muons to the number without muons, vs. jet shower energy. P_{nomu} is measured in the region above 400 GeV in the narrow jet shower data to be 0.11 ± 0.01 (black line). This is in fair agreement with the observed P_{nomu} in the wide-jet data (blue line).

VIII. BACKGROUND DETERMINATION

To estimate the number of wide no-muon showers expected from background, we use the assumption that the probability not to reconstruct the cosmic muon is independent of whether the muon shower is narrow or wide. Thus, we first measure the probability to miss the muon (P_{nomu}) in the narrow-jet cosmic data sample. Then this probability is applied to the wide-jet cosmic-muon data sample to predict the number (and energy spectrum) of wide-shower no-muon background events.

However, two complications must first be dealt with in the narrow-jet sample before we can measure P_{nomu} . First, there are hot spots (from detector problems or noise) that occur in the narrow-jet sample that are not manifested in the wide-jet data. This is understandable, since many detector problems and noise can be isolated to a single calorimeter cell or a small group of cells, and thus would lead only to narrow fake jets. These hot spots are removed from the narrow-jet sample before P_{nomu} is measured. A 2-dimensional histogram is made of the narrow-jet ϕ vs. η , and hot regions of this histogram (containing a number of events far exceeding the average) are excluded when measuring P_{nomu} . About 1% of the calorimeter area is excluded.

The second issue to be dealt with in the narrow-jet sample is contamination from beam-muons. The beam-muon events have different properties than the cosmic showers, due to their production mechanism and the angle that they tend to enter the detector from. Their energy spectrum is different from the cosmic showers, and falls off faster with energy (for instance, there are no showers above 1 TeV!). Because the beam-muons enter parallel to the beam-line, they can not readily induce showers with large ϕ -width, so they do not contribute significantly to the wide-jet events. And since they preferentially enter the detector near the far-forward region where muon acceptance is smaller, it is more likely to not reconstruct the muon in beam-muon events. For all of these reasons, it is critical to remove the contribution from beam-muons when measuring P_{nomu} .

We can fortunately study the properties of nearly-pure beam-muon showers whenever we do reconstruct the muon, since this muon is in-time ($|\Delta t| < 10$ ns) and the shower is near the plane of the beam. If we plot the fraction of in-time muons vs. energy, we see that the fraction decreases steadily vs. energy towards a plateau of about 5% above 400 GeV. If the muons were all of cosmic origin, and thus flatly distributed in time, the fraction of muons that randomly happened to be in-time would be 20 ns / 396 ns = 5%. (The $|\Delta t| < 10$ ns criteria implies a time window for in-time muons a total of 20 ns wide.) Thus, at high energy there is a negligible contribution from beam-muons. So we can measure P_{nomu} in the region above 400 GeV, as shown in Figure 5, and arrive at $P_{nomu} = 0.11 \pm 0.01$. The systematic uncertainty of the background is thus 10%.

Sample mass (GeV)	1 Jet	$ \eta <.9$	$E>90$ GeV	No PV	Width $<.25$	Width $>.08$	n90 ≥ 10	No good mu
200	0.91	0.91	0.30	0.98	1.00	0.57	0.85	1.00
300	0.87	0.89	0.97	0.97	1.00	0.50	0.86	0.96
400	0.83	0.89	0.99	0.96	0.99	0.56	0.89	0.97
500	0.81	0.91	0.99	0.97	0.99	0.56	0.85	0.97

TABLE I: The signal efficiencies for each cut, for each simulated gluino mass sample.

Source	Efficiency
GAPSN Trigger	.6
Trigger gaps	.68
Total	0.41

TABLE II: The extra signal inefficiencies, and their total product.

IX. SIGNAL EFFICIENCY

To first order, the detection efficiency for the stopped gluino signal events can be estimated from the MC simulation. The fraction of events falling outside the jet energy cuts, $|\eta|$ cut, n90 cut, and jet η -width and ϕ -width cuts can be fairly accurately predicted. Table I shows the efficiency for each criteria.

Some effects are not modeled in the MC. There is a loss of efficiency at the trigger level from the GAPSN requirement. If a min-bias event happens to occur during the bunch crossing when the gluino decays, the GAPSN trigger will not fire. The fraction of the time this occurs has been measured using cosmic-muon shower events triggered on the JT_125TT trigger from the ‘‘QCD’’ skim, which requires at least one jet above 125 GeV. 75% of the time that JT_125TT fired on a cosmic-muon shower the JT_45TT_GAPSN trigger also fired; thus the efficiency of the GAPSN trigger term, averaged over the data set, is 75%. The probability to have no min-bias interactions during a given crossing is proportional to $e^{-\lambda}$, where λ is the average number of interactions per crossing, which is proportional to the instantaneous luminosity. For this data set, $\lambda \simeq 0.3$. However, since it is more likely that the gluino decay occurs during a time close to its production compared to the length of a store, the inefficiency is actually higher. Since the gluino lifetime is unknown but presumed to be less than a few hours, the inefficiency is unknown, but we will conservatively estimate it to be $60 \pm 15\%$. In a worst case, if all the gluino decays occurred when the luminosity was twice that observed on average, the efficiency would be $.7^2 = 50\%$.

Another source of inefficiency is that the trigger is not live all the time, but only during the ‘‘live super-bunches’’. During the sync-gap and each of the two cosmic-gaps, the triggers are dead. (A trigger which fires during the cosmic gaps (21% of the turn) is under discussion for future use. It is not possible for $D\bar{O}$ to trigger during the sync gap (11% of the turn), when crate electronics are performing other tasks.) The live super-bunches make up 68% of the total accelerator turn time, with minimal uncertainty.

Finally, there is also a shift of the observed jet energy towards lower energies whenever the calorimeter signal from the gluino decay is not in-time with the bunch-crossing time. This is due to the fact that the calorimeter electronics sample the shaped calorimeter signal only once per bunch-crossing, at the assumed peak of the signal. The amount of inefficiency resulting can be measured by looking at cosmic-muon showers where the muon has been reconstructed. Very little falloff in efficiency can be seen vs. the muon time, as expected since the time window (up to only 50 ns, limited by the muon readout electronics) is short compared to where efficiency should start to drop (around 140 ns). So we need to measure the efficiency for muon showers outside this time window. The number of cosmic muon showers per ns above energy threshold outside the time window is 69% less than inside the window. This inefficiency corresponds to the average shower energy being decreased by 15%.

Table II shows the additional sources of inefficiency and the total efficiency to be multiplied by the MC acceptance. The uncertainties from all sources which affect the signal acceptance are added in quadrature, shown in Table III. The final signal efficiencies are shown in Table IV.

X. RESULTS

If we apply the measured P_{nomu} to the wide-jet cosmic-muon data sample, we can estimate the energy spectrum of the expected wide-jet no-muon background, as shown in Figure 6 along with the observed wide-jet no-muon events

Source	Uncertainty
Geometrical/Kinematic Acceptance	0.2
Min-bias Overlap	0.15
Total	0.25

TABLE III: The systematic uncertainties on signal efficiency, and their total (added in quadrature).

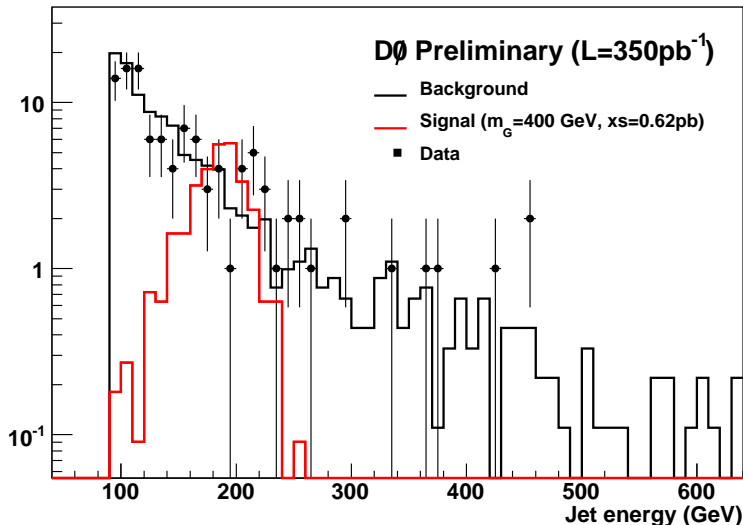


FIG. 6: A comparison of the wide-jet no-muon data (black points) to the expected background (black histogram), with log scale. Also shown is the signal simulated for $m_G=400$ GeV and $m_{LSP}=90$ GeV at the excluded limit of 0.7 pb (red histogram).

in data. The estimated background predicts the data well, and there is little excess in data at any energy range.

Given an observed number of candidate events, an expected number of background events, and a signal efficiency in a certain jet energy bin, we can exclude at 95% C.L. a calculated rate of signal events giving jets of that energy, taking systematic uncertainties into account. This is a fairly model-independent result, limiting the rate of any out-of-time mono-jet signal of a given energy. From there we can derive limits in the plane of $M_g - M_{LSP}$ for the stopped gluino model specifically.

The jet energy ranges chosen are calculated from the resolution of the simulated MC samples. The signal window for each of the four samples is from $M-0.5 \cdot \text{RMS} - M+2.0 \cdot \text{RMS}$, where M is the mean jet energy of the sample (after all selections) and RMS is the sample's jet energy RMS. Approximately 80% of the simulated signal events fell within this window cut, depending weakly on the signal mass. An asymmetric window was chosen since the background is falling exponentially with increasing jet energy, whereas the signal is roughly symmetric in jet energy around the mean. Table IV shows, for each jet energy range considered, the number of events observed in data, expected from background, the signal efficiency, and the corresponding observed and expected cross-section limits on signal jets. The integrated luminosity assumed was $350 \pm 20 \text{ pb}^{-1}$. These results are also shown in Figure 7.

From the relation between the gluino and LSP masses and the observed jet energy, Equation 1, one can solve for

Jet E Range (GeV)	Data	Bgnd.	Signal Efficiency	Exp. Limit (pb)	Obs. Limit (pb)
94.6-111.6	46	48.18	0.05	1.39	1.27
126.8-171.8	32	37.84	0.10	0.59	0.45
169.3-233.8	27	21.56	0.11	0.40	0.62
214.2-286.6	14	9.57	0.10	0.30	0.52

TABLE IV: The data, background, efficiency, and observed and expected limits (at 95% C.L.) for each jet energy range.

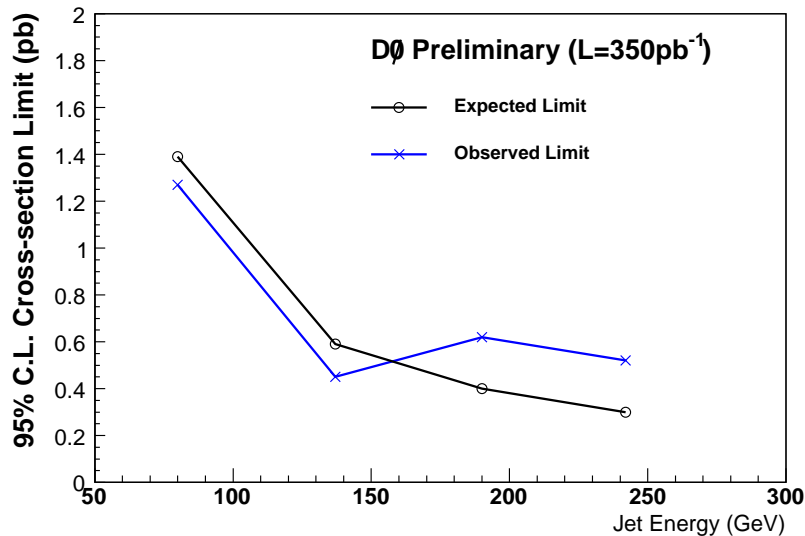


FIG. 7: The 95% C.L. upper limits expected (black, open circles) and observed (blue, filled circles) on the cross-section of stopped particles decaying into a jet within various energy ranges.

the gluino mass:

$$M_g = E + \sqrt{E^2 + M_{LSP}^2} \quad (2)$$

Using this equation, results can be translated from the generated set of signal samples to any other set of (M_g, M_{LSP}) which would give the same generated parton (jet) energy. For example, one of the generated samples had $M_g=400$ GeV and $M_{LSP}=90$ GeV. (All of the generated samples had $M_{LSP}=90$ GeV, which corresponds to the Z mass). This sample corresponds to a parton (jet) energy of 190 GeV, as given by Equation 1. If instead M_{LSP} had been chosen to be 200 GeV, an equivalent jet energy could have been simulated by having M_g be 466 GeV, according to Equation 2.

We can now place upper limits on the stopped gluino cross-section $\times \text{BR}(G \rightarrow g\chi_1^0)$ vs. the gluino mass, for an assumed LSP mass. These can be compared with the predicted cross-sections for stopped gluinos (which includes its production and its probability to stop) taken from [3]. Figure 8 shows the gluino cross-sections $\times \text{BR}(G \rightarrow g\chi_1^0)$ excluded for assumed LSP masses of 50, 90, and 200 GeV.

XI. DISCUSSION

This is the first experimental study for this type of signal at a hadron collider. The results from 350pb^{-1} of Tevatron data are able to exclude a gluino mass below about 270 GeV, for a light neutralino. Much experience has been gained with the analysis methods and backgrounds involved. Additional integrated luminosity, new triggers, and improved background rejection should allow for much greater sensitivity at the Tevatron in the near future. Experiments at the nearly completed LHC, due to begin operation in 2007, will also offer a prime environment to carry out a similar analysis, due to the larger beam energy, luminosity, shielding from cosmic radiation, and detector capabilities.

Acknowledgments

Thanks to Jay Wacker for very helpful discussions. We thank the staffs at Fermilab and collaborating institutions, and acknowledge support from the DOE and NSF (USA), CEA and CNRS/IN2P3 (France), FASI, Rosatom and RFBR (Russia), CAPES, CNPq, FAPERJ, FAPESP and FUNDUNESP (Brazil), DAE and DST (India), Colciencias (Colombia), CONACyT (Mexico), KRF (Korea), CONICET and UBACyT (Argentina), FOM (The Netherlands), PPARC (United Kingdom), MSMT (Czech Republic), CRC Program, CFI, NSERC and WestGrid Project (Canada), BMBF and DFG (Germany), SFI (Ireland), A.P. Sloan Foundation, Research Corporation, Texas Advanced Research

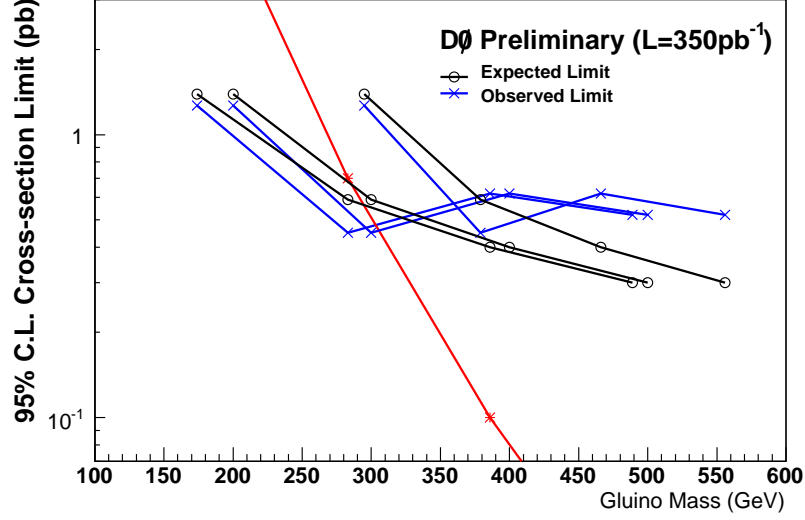


FIG. 8: The 95% C.L. upper limits expected (black, open circles) and observed (blue, crosses) on the cross-section of stopped gluinos decaying into a jet plus LSP, for 3 assumed LSP masses: 50, 90, and 200 GeV. The larger the LSP mass assumed, the larger the gluino mass needed for the same cross-section limit. Also shown is the theoretical cross-section (red, stars), from [3].

Program, Alexander von Humboldt Foundation, and the Marie Curie Fellowships.

-
- [1] N. Arkani-Hamed, S. Dimopoulos, G. F. Giudice and A. Romanino, Nucl. Phys. B **709**, 3 (2005) [arXiv:hep-ph/0409232].
 [2] A. C. Kraan, Eur. Phys. J. C **37**, 91 (2004) [arXiv:hep-ex/0404001].
 [3] A. Arvanitaki, S. Dimopoulos, A. Pierce, S. Rajendran and J. Wacker, arXiv:hep-ph/0506242.
 [4] G. C. Blazey *et al.*, in *Proceedings of the Workshop: "QCD and Weak Boson Physics in Run II,"* edited by U. Baur, R. K. Ellis, and D. Zeppenfeld, (Fermilab, Batavia, IL, 2000) p. 47; see Sec. 3.5 for details.